Gas sorption and transport in coals: A poroelastic medium approach

Jun Yi [a], I.Yücel Akkutlu [b,*], C.Özgen Karacan [c], C.R. Clarkson [d]

[a] Chongqing University, Chongqing, China
[b] University of Oklahoma, Norman, USA
[c] CDC, NIOSH, Pittsburgh Research Laboratory, Pittsburgh, USA
[d] University of Calgary, Calgary, Alberta, Canada

A B S T R A C T

In this paper, single-component gas sorption and transient diffusion processes are described within coal matrix exhibiting bimodal pore structure. The coal matrix is treated as a poroelastic medium manifesting swelling and shrinkage effects due to the sorption of gas under effective overburden stress. Gas transport is considered Fickian with molecular (bulk) and surface diffusion processes simultaneously taking place in the macro- and micropores of coal, respectively. The numerical formulation is intended to be explicit in nature to investigate the influences of sorption phenomena on the macropore volumes and on the overall gas transport for the cases of gas uptake by and release from coal.

Results of the study show the presence of hysteresis during a sorption–desorption cycle of the gas. It is also found that the overall gas transport takes place at a rate significantly less than that in the macropores only. Thus the existence of a retardation effect in the overall gas transport is concluded. This retardation effect is primarily due to the micropore resistances, in particular gas adsorption, and is independent of the changes in the macropore volumes. It is shown that macroporosity of the coal matrix may change during gas transport due to combined effects of pressure and sorption-induced swelling or shrinkage of the coal. It is estimated that the macroporosity variation is non-uniform in space and time, as it is expected in reality, and typically taking values less than ±10 percent of the initial porosity.

1. Introduction

As an unconventional natural gas resource, coalbed methane receives worldwide attention. Coal seam gas is produced using methods and technologies adapted from the conventional oil and gas industry. Both primary (pressure) depletion and enhanced coalbed methane recovery (ECBM) methods have been tested for different pilot scales. In the ECBM process, non-hydrocarbon gases (e.g., flue gas, nitrogen or carbon dioxide) are injected to improve recovery of CH_4, either by stripping (e.g. with nitrogen) or displacement (e.g. with CO_2). In the case of displacement with CO_2 injection, one additional benefit is to simultaneously sequester CO_2, if the geology and hydrology of the coalbed permit long term storage of injected gas.

Unlike conventional reservoirs, gas storage, flow and transport processes in coal seams are quite complex, mainly due to the extremely intricate and heterogeneous nature of the coal. Coals exhibit multi-scale heterogeneity often characterized by a distinctive matrix structure involving macropores and micropores (Gan et al., 1972; Unsworth et al., 1989), which can be treated with a bimodal (bidisperse) pore size distribution. The matrix-pore structure, specifically the relative abundance of micro-/meso-/macropores volume, has been demonstrated to be a function of coal organic matter composition and thermal maturity (ex. Gan et al., 1972; Clarkson and Bustin, 1999a).

Coal can be viewed as a solid, organic microporous material hosting micropores, interconnected macropores and uniformly distributed fractures, i.e., cleats. Most gas storage occurs within the microporous matrix, which has a large internal surface area; mass transfer is primarily by diffusion. On the other hand, large fractures and cleats penetrating the coal matrix have very limited gas storage capacity but they are important for their role in Darcian flow of gas and water, and thus in production and injection operations. Hence, at moderate to high coalbed pressures a significant amount of natural gas resides on the surfaces of micropores in an adsorbed state (Thimons and Kissel, 1973), as well as in intra-molecular voids within complex macromolecular structure of the solid material in an absorbed/dissolved state (Karacan, 2003; Larsen, 2004; Romanov et al., 2006; Medek et al., 2006).

Gas adsorption and dissolution may cause the coal matrix to swell and/or shrink. This may change the specific surface areas and total macropore volume of the coal matrix (Romanov et al., 2006), and thus gas transport by diffusion in the coal matrix (Cui et al., 2004; Yi et al., 2008). Also, the change in the matrix volume may vary the cleat aperture width which in turn may affect the Darcian flow to the boreholes by changing the effective permeability of coal. Therefore, during primary

* Corresponding author. 100 East Boyd, Sarkeys Energy Center, Room T-311, Norman, OK 73079-1003, USA. Tel.: +1 405 325 8141; fax: +1 405 325 7477.
E-mail address: akkutlu@ou.edu (I.Y. Akkutlu).

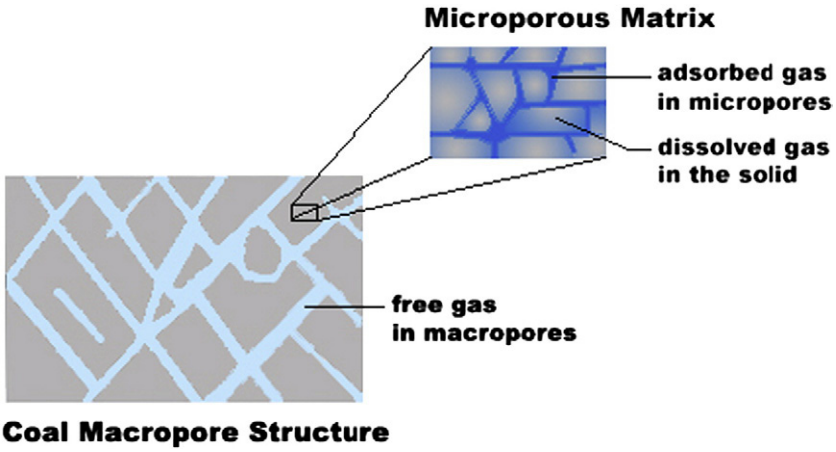

Fig. 1. Schematic of bidisperse coal pore structure showing macro- and micropores containing gas in free, adsorbed and dissolved states.

production and ECBM operations, adsorption and dissolution processes are anticipated to add a complex and dynamic nature to production and injection operations. Thus, depending on the combined effects of gas sorption and the effective stress variations, the absolute permeability of coal may change during primary depletion or greenhouse gas sequestration/enhanced recovery (ECBM) operations (Palmer and Mansoori, 1998; Shi and Durucan, 2005).

Based on the premise that the injection and production operations are controlled by flow through cleats and the interconnected fractures, a series of experimental (Harpalani and Schraufnagel, 1990; Seidle et al., 1992), theoretical (Palmer and Mansoori, 1998; Cui and Bustin, 2005; Shi and Durucan, 2005; Mavor and Gunter, 2006) and field (Gierhart et al., 2007; Clarkson et al., 2008) studies were reported in literature to investigate the overall influences of the adsorbed gas and effective stress on cleat permeability, particularly around wellbore. Although, these pioneering studies improved our understanding of the possible causes of permeability changes around the borehole, they did not attempt to separate out the effects of absorption and adsorption and ignored the effect of dissolved gas in the coal matrix on permeability evolution. Consequently, they may have simply attributed the swelling effect entirely to adsorption. In addition, they did not consider the effect of macropore changes in the coal matrix on diffusive transport.

Smith and Williams (1984), Clarkson and Bustin (1999b), Shi and Durucan (2003), Cui et al. (2004), and Yi et al. (2008) among others, previously applied some form of a bidisperse model to describe CH_4, N_2, or CO_2 transport through the coal matrix. Smith and Williams (1984) applied Ruckenstein et al.'s (1971) analytical model assuming linear adsorption of CH_4 in both micro- and macropores, whereas the latter authors used numerical methods to quantify diffusion through micro-/macropores, assuming non-linear adsorption in the micropores. None of these studies considered storage due to absorption.

The purpose of this paper is to develop a theoretical framework suitable for a fundamental investigation of single-component gas sorption and transport in the coal matrix, which shows poroelastic material behavior. In this paper, a bidisperse coal structure viewed as a microporous matrix, which contains pores on the order of a few molecular diameters, penetrated throughout by interconnected macropores (Fig. 1) was considered. It was conceptualized that the microporous matrix retains the bulk of the gas, while the macropores have relatively negligible gas sorption capacity compared to micropores. In addition, since the matrix exhibits a large internal surface area for gas sorption and a relatively strong affinity for gas, it is expected that an additional diffusive mass transport in the adsorbed phase develops in the direction of free gas mass fluxes. Thus, it is assumed that gas sorption rates and flow in and out of coal are controlled by combined pore and surface diffusive mass fluxes. Furthermore, the sorbed and free gas mass-transport processes are expected to vary spatially and temporally and they can be mapped by mathematical models. The so-called "dual-sorption" approach is considered for the modeling of adsorption and dissolution. The approach invokes the existence of two thermodynamically distinct gas populations, namely, molecules dissolved in the solid coal material by an ordinary dissolution mechanism (obeying Henry's law) and the molecules residing in the preexisting openings, i.e., micropores, in the matrix (obeying Langmuir type of isotherm) with rapid exchange between these two populations (Rangarajan et al., 1984). An early development and illustration of the applicability of the dual sorption model are a result of extensive investigations by Koros et al. (1977), Chan et al. (1978), Erb and Paul (1981) on sorption and transport of gases in glassy polymers. An exhaustive review by Paul (1979) furnishes detailed information pertaining to different aspects of dual sorption model. Later, the dual sorption model has been applied to describe solvent (Green and Selby, 1994,) and organic vapor sorption behaviors in coals (Shimuzu et al., 1998).

2. Sorption and Transport in Poroelastic Coal

In this section, the governing equations are described in one-dimension and in scaled and dimensionless forms. It is shown that the description can be achieved using a nonlinear second order transient-diffusive gas mass conservation equation coupled with two auxiliary equations — those that describe the dynamics of solid/pore volume change and the equilibrium sorption isotherm.

For the solution of the governing equations describing the fundamentals of gas sorption and transport in coal, the conceptual coal matrix block is subjected to initial and boundary conditions so that gas uptake and release experiments can be performed numerically to investigate the influence of adsorbed/dissolved gas on the microporous matrix and macropore volumes. The results are presented using the estimated fractional uptake and release rates, the macroporosity variations and, as an indication of overall gas transport, the apparent diffusion coefficient.

With Eq. (1) the continuum description is considered valid and, hence, at a given time and location, gas is distributed at adsorbed and dissolved states in the microporous coal matrix and as free gas in the macropores. Gas mass balance in one-dimensional bidisperse coal contains the following transient and diffusive terms:

$$\frac{\partial}{\partial t}(\phi C)+\frac{\partial}{\partial t}\left[(1-\phi)C_\mu\right]=\frac{1}{x^n}\frac{\partial}{\partial x}\left(x^n\phi D_p\frac{\partial C}{\partial x}\right)+\frac{1}{x^n}\frac{\partial}{\partial x}\left(x^n(1-\phi)D_s\frac{\partial C_\mu}{\partial x}\right) \quad (1)$$

In this equation, n is the shape factor for the coal body (where $n=0$ for linear, $n=1$ for cylindrical and $n=2$ for spherical coordinates). C is

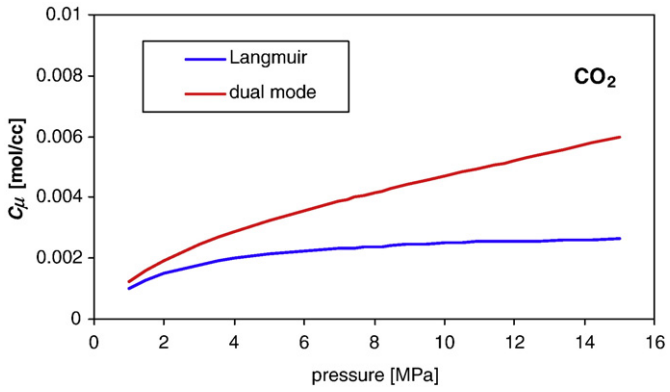

Fig. 2. Comparison of the Langmuir–Henry "dual-mode" sorption isotherm, i.e., Eq. (2), with the Langmuir adsorption isotherm. The pressures are obtained using ideal gas law.

the free gas concentration in the macropores (moles per unit macropore volume), whereas C_μ represents concentration of the gas sorbed by the microporous solid (moles per unit microporous matrix volume). The first terms on both sides of the governing equation include a macroporosity ϕ describing gas mass accumulation and diffusive mass flux in the macropore void space, respectively. The second terms, including $(1-\phi)$, represent the accumulation and transport of the sorbed gas in the microporous matrix.

It should be noted that only the total amount of sorbed gas enters in the mass balance given in Eq. (1) and that its transport through the microporous matrix is considered to obey Fick's law. Thus, using Deborah Number, $De=\alpha/\theta$ introduced by Vrentas et al. (1975) and Vrentas and Duda (1977), with the Eq. (1), it is implicitly assumed that the macromolecular structural relaxation time α is either much larger ($De\gg1$) or much smaller ($De\ll1$) than characteristic diffusion time, θ. When De is in the order of one, on the other hand, the microporous coal matrix changes phase from glassy structure to rubbery structure in the presence of a sharp moving boundary. Consequently, a diffusion process that starts out as Fickian may turn into a so-called Case II, or anomalous diffusion, with a shock front (Thomas and Windle, 1982; Neogi 1983; Hui et al., 1987). However, Mazumder and Bruining (2007) recently showed that, in practice, the latter could only be a transitional effect for the gas–coal systems. This type of anomalous behavior is therefore not considered in this work.

In addition, in the development of a mathematical description, the microporous matrix is considered to be in equilibrium with the gas and its equilibrium sorption dynamics is described with the Langmuir–Henry dual-mode isotherm (Green and Selby, 1994; Shimuzu et al., 1998). If $C_{\mu s}$ represents the complete monolayer coverage in the solid–gas interface and k'_d the coefficient of linear absorption, then the isotherm can be described as:

$$C_\mu = \frac{C_{\mu s} b' C}{1+b'C} + k'_d C \tag{2}$$

Here $b'=bRT$ and b is often referred to as the Langmuir constant. When the total gas pressure p is low (i.e., $bp\ll1$), Eq. (2) reduces to a form similar to Henry's law isotherm, which states that the sorbed gas concentration in the microporous solid increases linearly with the gas pressure. The dual-mode isotherm model is an effective approach to match laboratory experiments, particularly for glassy polymers. This approach has also been used to investigate organic vapor solvent–coal interactions (Medek et al., 2006) with the assumptions in the transport equation describing organic vapor–coal interactions, such as the two modes are in equilibrium and take place simultaneously; gas molecules adsorbed under Langmuir mode are immobilized; and diffusion occurs only in the dissolved mode and the diffusion coefficient is independent of concentration.

Fig. 2 shows a comparison of the dual mode equilibrium sorption isotherm (Eq. (2)) with the Langmuir adsorption isotherm versus pressure, i.e., the free gas macropore concentration C. The values of pressure in this figure are obtained using the ideal gas law. The dual-mode isotherm implies that the gas sorption increases infinitely with pressure. Thus, although for the pressure ranges of relevance for CBM and CO_2-ECBM scenarios this model yields sorption isotherms that are typical, the consequence of applying this relationship uncritically may yield highly unrealistic sorption values for coals. Numerical experiments reported in this work are in between 0–5 MPa, i.e., the lower end of the pressure domain shown above.

In order to include macropore-volume strain changes into the overall transport model, linear elasticity for strain changes in isothermal coal is considered. For this purpose, Palmer and Mansoori's (1998) poroelastic model is modified to describe the macropore-volume strain increments under the influence of sorption and constant overburden stress:

$$d\phi = \left[a_1 + a_2 + a_3 \frac{b'}{(1+b'C)^2}\right] dC \tag{3}$$

The coefficients, a_i, in Eq. (3) represent the stress and sorption-induced volumetric strains:

$$a_1 = \left[\frac{RT}{M} - \left(\frac{K}{M}-1+f\right)\gamma RT\right]; \quad a_2 = \left(\frac{K}{M}-1\right)k'_d; \quad a_3 = \left(\frac{K}{M}-1\right)\varepsilon_l$$

Eq. (3) is slightly different from the form originally proposed in that it now explicitly includes the effect of dissolved gas in solid material. It is developed based on the common assumption (Cui and Bustin, 2005) that the shape of the volumetric strain-sorbed gas concentration curve is a Langmuir–Henry isotherm of the form given in Eq. (2). ε_l represents a dimensionless adjustment parameter for the strain and adsorbed gas concentration. The terms on the right side of Eq. (3) are referred to as the macropore compression (a_1) effect, microporous shrinkage/swelling effects due to dissolution (a_2) and adsorption (a_3), respectively.

Inserting Eqs. (2) and (3) and expanding the terms in Eq. (1), and by applying the chain rule of differentiation, the following form of Eq. (1) is obtained for gas sorption and transport in coal particles exhibiting volumetric strain. In this development concentration-independent diffusion coefficients are assumed.

$$\left[\phi + (1-\phi)\frac{\partial C_\mu}{\partial C} + (C-C_\mu)\frac{\partial \phi}{\partial C}\right]\frac{\partial C}{\partial t} = \left(\frac{\phi D_p}{x^n}\right)\frac{\partial}{\partial x}\left(x^n\frac{\partial C}{\partial x}\right) + \left(\frac{(1-\phi)D_s}{x^n}\right)\frac{\partial}{\partial x}\left(x^n\frac{\partial C_\mu}{\partial C}\frac{\partial C}{\partial x}\right) + \left(D_p - D_s\frac{\partial C_\mu}{\partial C}\right)\frac{\partial \phi}{\partial C}\left(\frac{\partial C}{\partial x}\right)^2 \tag{4}$$

where $\partial\phi/\partial C$ and $\partial C_\mu/\partial C$ can be described explicitly using Eqs. (2) and (3):

$$\frac{\partial \phi}{\partial C} = a_1 + a_2 + a_3\frac{b'}{(1+b'C)^2} \quad \text{and} \quad \frac{\partial C_\mu}{\partial C} = \frac{C_{\mu s} b'}{(1+b'C)^2} + k'_d.$$

The second term on the right hand side of Eq. (4) can further be expanded to yield:

$$\left[\phi + (1-\phi)\frac{\partial C_\mu}{\partial C} + (C-C_\mu)\frac{\partial \phi}{\partial C}\right]\frac{\partial C}{\partial t} = \left[\phi D_p + (1-\phi)D_s\frac{\partial C_\mu}{\partial C}\right]\frac{1}{x^n}\frac{\partial}{\partial x}\left(x^n\frac{\partial C}{\partial x}\right) + \left[\left(D_p - D_s\frac{\partial C_\mu}{\partial C}\right)\frac{\partial \phi}{\partial C} + (1-\phi)D_s\frac{\partial^2 C_\mu}{\partial C^2}\right]\left(\frac{\partial C}{\partial x}\right)^2$$

Dividing each term by the coefficient of free gas accumulation (i.e., the terms inside the brackets on the left hand side) gives the gas mass balance in the following simplified form:

$$\frac{\partial C}{\partial t} = \overline{D}(C)\frac{1}{x^n}\frac{\partial}{\partial x}\left(x^n\frac{\partial C}{\partial x}\right) + \overline{f}_S(C)\left(\frac{\partial C}{\partial x}\right)^2 \tag{5}$$

In Eq. (5), the only dependent variable is the free gas concentration $C(x,t)$ in the macropores.

Eq. (5) contains two nonlinear coefficients: D and f_s, which are described as:

$$\overline{D}(C) = \frac{1}{\Delta_{\text{retard}}}\left[\phi D_p + (1-\phi) D_s \frac{\partial C_\mu}{\partial C}\right] \tag{6a}$$

and,

$$\overline{f}_S(C) = \frac{1}{\Delta_{\text{retard}}}\left[\left(D_p - D_s\frac{\partial C_\mu}{\partial C}\right)\frac{\partial \phi}{\partial C} + (1-\phi) D_s \frac{\partial^2 C_\mu}{\partial C^2}\right], \tag{6b}$$

$$\Delta_{\text{retard}} = \phi + (1-\phi)\frac{\partial C_\mu}{\partial C} + (C - C_\mu)\frac{\partial \phi}{\partial C}. \tag{6c}$$

As an immediate consequence of the formulation of the conceptual model, these equations suggest that diffusive gas transport in bimodal coal structure is always under the influence of a retardation effect (Eq. (6c)) during equilibrium sorption phenomena. Although the latter varies with the effects of free gas amount on the adsorbed phase and on the macroporosity, it takes values larger than unity during gas sorption and desorption, therefore, the effective gas transport is expected to be at a lower rate compared to gas transport in the macropores (unipore structure) only.

By employing Eqs. (2) and (3) in Eqs. (6a) and (6c), apparent diffusion coefficient, D, in the coal and the retardation effect can be described simultaneously as:

$$\overline{D}(C) = \frac{1}{\Delta_{\text{retard}}}\left[\left(\phi D_p + (1-\phi)\frac{C_{\mu s} b'}{(1+b'C)^2} + k'_d\right) D_s\right], \tag{7a}$$

$$\Delta_{\text{retard}} = \phi + (1-\phi)\left[\frac{C_{\mu s} b'}{(1+b'C)^2} + k'_d\right] + \left(C - \frac{C_{\mu s} b' C}{1+b'C} - k'_d C\right)\left[a_1 + a_2 + a_3\frac{b'}{(1+b'C)^2}\right], \tag{7b}$$

In summary, Eqs. (5) and (6b) together with Eqs. (7a), (7b) describe the transient gas sorption and transport in poroelastic coal with bidisperse pore structure in terms of the free and sorbed gas concentration.

2.1. Scaling and Nondimensionalization

Prior to defining the initial and boundary conditions and to obtaining numerical solutions, Eq. (5) was transformed to the following dimensionless form.

$$\frac{\partial c}{\partial \tau} = D(c)\frac{1}{r^n}\frac{\partial}{\partial r}\left(r^n\frac{\partial c}{\partial r}\right) + f_S(c)\left(\frac{\partial c}{\partial r}\right)^2 \tag{8}$$

The following nondimensional variables are introduced in Eq. (8):

$$r = \frac{x}{L}; \qquad \tau = \frac{D_p t}{L^n}; \qquad c = \frac{C}{C_o + C_{\mu o}}$$

where L corresponds to a characteristic coal sample length defined as the half-length of a symmetric coal slab in linear geometry (i.e., the shape factor n equal to zero). C_o and $C_{\mu o}$ are the initially available free and sorbed gas concentrations, respectively. The dimensionless coefficients of Eq. (8) are

$$D(c) = \frac{1}{\Delta}\left[\left(1 + \varepsilon\left(\frac{1-\phi}{\phi}\right)\frac{\lambda_{\mu s}}{(1+\lambda c)^2} + k'_d\right)\right], \tag{9a}$$

$$f_S(c) = \frac{1}{\Delta}\left[\left(1-\varepsilon\frac{\lambda_{\mu s}}{(1+\lambda c)^2} + k'_d\right)\right)\left(a'_1 + a'_2 + a_3\frac{\lambda}{(1+\lambda c)^2}\right)\left(+\varepsilon\left(\frac{1-\phi}{\phi}\right)\frac{2\lambda_{\mu s}\lambda}{(1+\lambda c)^3}\right)\right] \tag{9b}$$

where

$$\Delta = 1 + \left(\frac{1-\phi}{\phi}\right)\left[\frac{\lambda_{\mu s}}{(1+\lambda c)^2} + k'_d\right]\left(+\frac{1}{\phi}\left(c - \frac{\lambda_{\mu s} c}{1+\lambda c} - k'_d c\right)\left[a'_1 + a'_2 + a_3\frac{\lambda}{(1+\lambda c)^2}\right]\right) \tag{9c}$$

where the dimensionless quantities are:

$$\varepsilon = \frac{D_s}{D_p}; \qquad a'_i = a_i(C_o + C_{\mu o}); \qquad \lambda = b'(C_o + C_{\mu o}); \qquad \lambda_{\mu s} = C_{\mu s} b'$$

Eq. (8) is a second order nonlinear partial differential equation, numerical approximation of which could be obtained using an implicit finite difference scheme and Newton iteration. Time integration of the ordinary differential equations resulting from the discretization in space is performed by a solver, which is based on an implicit linear multi-step method that chooses the time steps dynamically during the computations (Higham and Higham, 2005).

2.2. Initial/Boundary Value Problems

Gas sorption and transport within a coal particle that experiences strain due to sorption/desorption, overburden stress and gas dissolution in the matrix are investigated based on solutions to Eq. (8) using the initial and boundary conditions given in Table 1. This table indicates that initially gas is either absent (in the case of uptake) or distributed uniformly (in the case of release) as free gas in macropores and in sorbed states in the microporous matrix as dictated by the dual-mode sorption isotherm. The outer boundary condition (at $r=1$) is described as a source/sink for the gas. Although, the conditions are defined for the free gas concentration in the macropores, amounts of the adsorbed dissolved gas at any particular time and location can be easily predicted at each time step.

The properties of gas–coal system are given in Table 2. The investigation considers the sorption and transport behavior comparatively for CH_4, N_2 and CO_2 separately. As shown in Table 2b, we consider that these components have preferential and graded sorption tendencies with the coal such that CO_2 has the largest, CH_4 the intermediate and N_2 the smallest sorption capacity. Henry's constant

Table 1
Initial/boundary value problems

Gas uptake:	Gas release:
$\tau=0$; $c(r,0)=0$	$\tau=0$; $c(r,0)=1$
$r=0$; $\partial c/\partial r=0$	$r=0$; $\partial c/\partial r=0$
$r=1$; $c=1$	$r=1$; $c=0$

Table 2
Properties of gas and coal materials

Parameter	Unit	Value
A — Coal Properties		
Temperature, T	°K	293.0
Initial macroporosity, ϕ	frac.	0.02
K/M ratio	frac.	0.54
Parameter, f	frac.	0.50
Grain compressibility, γ	1/MPa	1.3E-10
Initial free gas conc., C_o	moles/cc	2.0E-03

Parameter	Unit	Value		
		N_2	CH_4	CO_2
B — GAS PROPERTIES				
$C_{\mu s}$	mole/cc	2.0E-3	2.5E-3	3.0E-3
b'	cc/mole	5.0E+2	8.0E+2	12.0E+2
k'_d	frac.	8.0E-2	28.0E-2	54.0E-2
ε_l	frac.	9.0E-3	12.3E-3	24.6E-3
$\varepsilon = D_s/D_p$	frac.	1.0E-3	1.0E-3	1.0E-3

k'_d values estimated for these components are 0.54, 0.28, and 0.008, respectively (Medek et al., 2006).

3. Results and Discussion

3.1. Fractional Gas Uptake/Release Rates

Fig. 3 shows free CH_4 and CO_2 fractions in the coal sample as a function of dimensionless time during gas sorption and desorption stages. Hysteresis observed between sorption and desorption curves points to a complex interplay of the processes describing solid–gas interactions under different initial conditions. The adsorption hysteresis has a long history (Cohan, 1938); however, the existing discussion in the literature involves its association with the occurance of capillary condensation, a phenomenon which is not considered in our model. Desorption curves show that almost all of the gas in adsorbed and dissolved phases is eventually being desorbed under the influence of the existing concentration gradients across the coal sample at longer times.

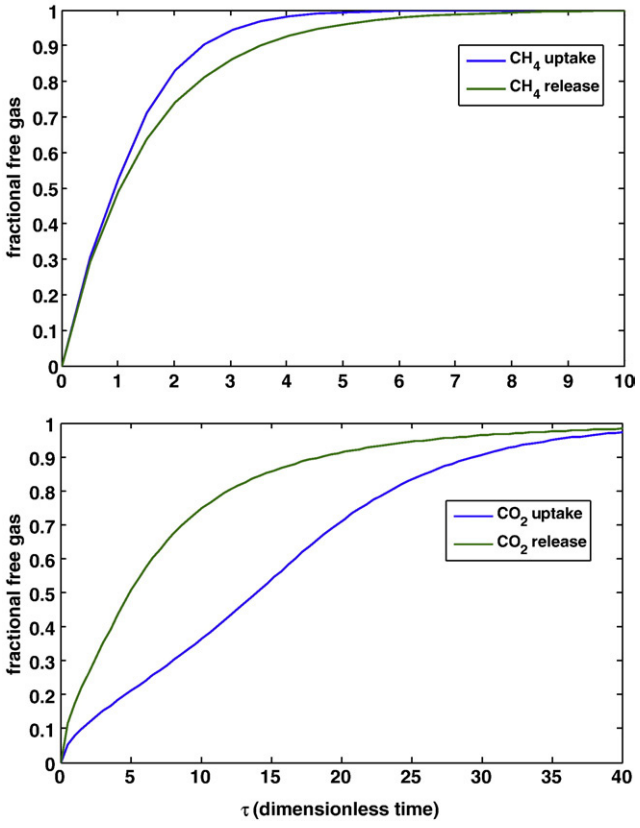

Fig. 3. Fractional gas uptake and release for CH_4 and CO_2. (Blue lines are the fraction of gas desorbed, whereas green lines are the fraction of gas adsorbed.)

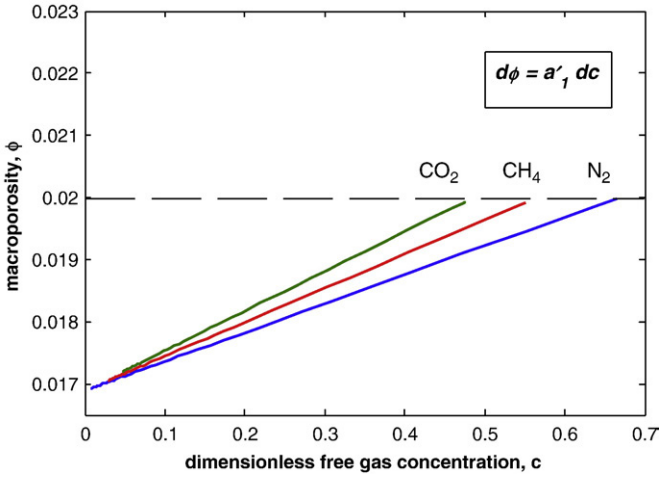

Fig. 4. Estimated macroporosity versus free gas concentration at $r=0.5$ during gas release from coal. Initial macroporosity is 2%. Porosity variations are due to overburden stress only, i.e., $a_1 \neq 0$, $a_2 = 0$, $a_3 = 0$.

We note that the x-coordinate in Fig. 3 is dimensionless time τ, which is normalized using D_p, defined as macropore diffusivity in the manuscript. Based on the previous experimental studies to date, the latter is expected to take larger values for CO_2. Hence, if we were to convert the x-coordinate to dimensional time t using lower macropore diffusivity value for CH_4 in Fig. 3a and higher value for CO_2 in Fig. 3b, then the real time scale for methane would stretch significantly. According to Clarkson and Bustin (1999b) and Cui et al. (2004), we anticipate that this stretching will cause the CH_4 sorption to take place in a time scale ten to hundred times longer than the times scale for CO_2.

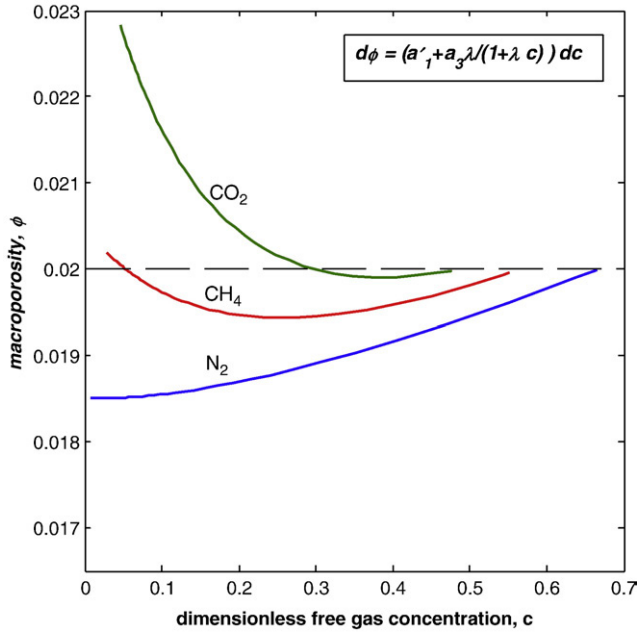

Fig. 5. Estimated macroporosity versus free gas concentration at $r=0.5$ during gas release from coal. Initial macroporosity is 2%. Porosity variations are due to $a_1 \neq 0$, $a_2 = 0$, $a_3 \neq 0$.

3.2. Influence of Sorption on Coal Macroporosity

As described previously in Eq. (3), changes in coal macroporosity during gas sorption and transport are due to three independent effects. Figs. 4–6 show these effects separately during gas desorption from coal.

Fig. 4 shows the influence of only a constant overburden stress on the macroporosity as a linear pore-volume compression effect. Using this analysis $d\phi/dc$ is estimated to be a positive value and changing linearly as a function of free gas concentration, or with pore pressure. Furthermore, when free gas concentration in the coal drops to zero, macroporosity decreases from its initial value of 2% to a lower value of 1.7%. The convergence to the same porosity value is expected for all gases since the intrinsic properties of the gases and their interactions with coal during sorption are excluded at this stage. The macroporosity change is only due to the gas concentration, thus pore pressure, change.

In Fig. 5, the influence of adsorption is introduced in addition to the previous analysis, i.e, $a_2=0$, whereas $a_1\neq0$ and $a_3\neq0$. Fig. 5 shows the adsorption isotherm-related deviations from the linearity previously illustrated in Fig. 4. Depending on the adsorption capacity of coal, each component shows a different effect on macroporosity changes during the gas release. As lower concentrations are reached, desorption-related coal shrinkage effect becomes somewhat more dominant in N_2. However, in the case of CO_2 and CH_4 a decrease in macropore porosity is experienced during desorption when pressure (or concentration) decreases, followed by an increasing period during which porosity re-bounds back to values higher than initial porosities showing more shrinkage taking place. Thus, the porosity increase due to shrinkage effect overcomes porosity decrease due to increasing compression effect during desorption. The final porosities depend on the interplay of these two and the adsorption affinities of the gases.

In the next step of the analysis, the influence of gas absorption (or dissolution) is investigated during the gas desorption experiments, i.e., $a_2\neq0$ is also taken. Fig. 6 shows the combined effects of sorption (adsorption and absorption) processes and overburden stress on macroporosity. This figure clearly shows that previous observations in Fig. 5 are amplified when the effect of gas dissolution in the coal matrix is included. Dissolved gas apparently causes matrix to shrink more, compared to adsorption only, during a gas-release process. A re-bound effect is observed where macroporosity first decreases due to pressure effects, then increases as a result of matrix-shrinkage; in the case of CH_4 and CO_2, the macroporosity at low concentrations actually exceeds the initial macroporosity. For example, when the dimensionless CH_4 amount drops to ~0.15, the decrease of porosity due to increasing overburden stress is balanced by increased shrinkage of the coal matrix and a re-bound effect around 1.9% porosity is observed.

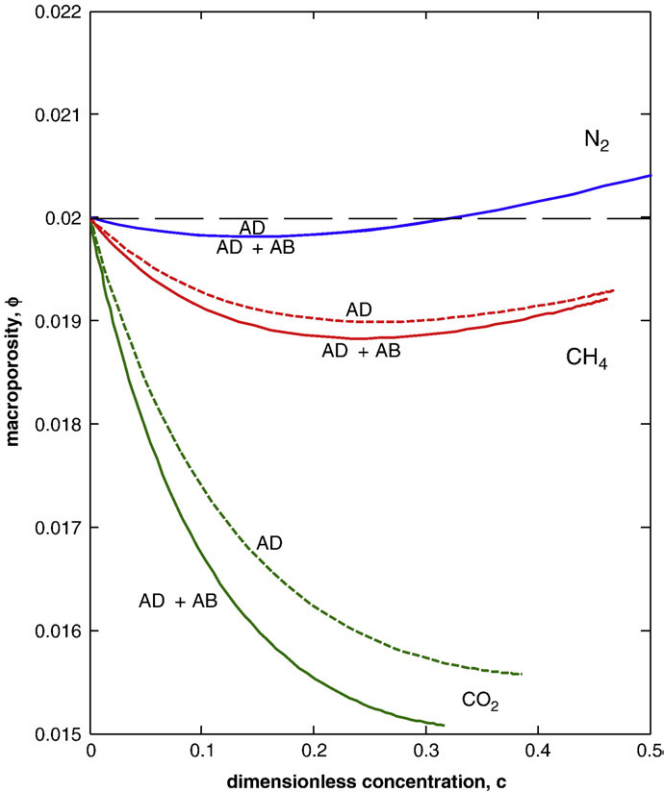

Fig. 7. Estimated macroporosity versus free gas concentration at $r=0.5$ during gas uptake by coal. Solid lines with full model; dashed lines with gas adsorption only.

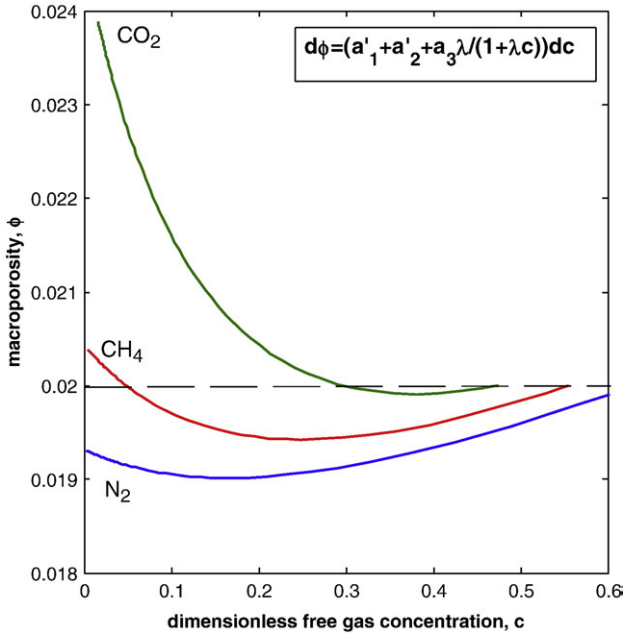

Fig. 6. Estimated macroporosity versus free gas concentration at $r=0.5$ during gas release from coal. Porosity variations due to varying a_1, a_2, a_3 coefficients.

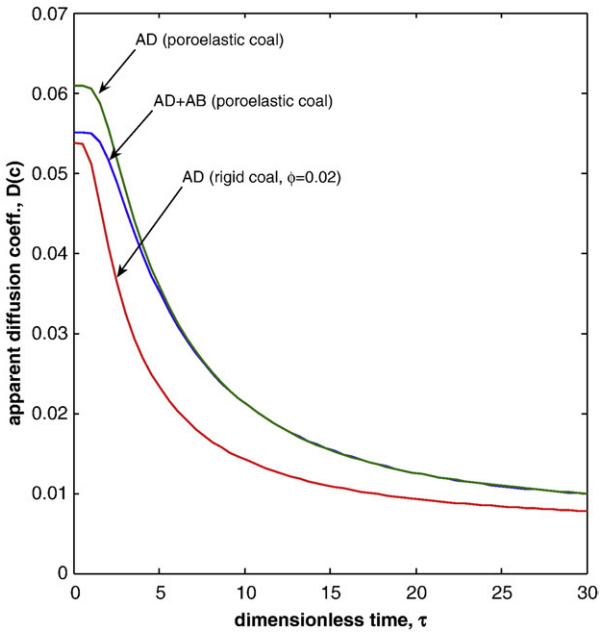

Fig. 8. Dimensionless apparent diffusion coefficient $D(c)$ versus time during CO_2 release from bidisperse coal. The coefficient is normalized using the macropore pore diffusion coefficient, D_p.

The presence of a gas dissolution mechanism creates additional shrinkage/swelling effects on macroporosity for N_2 and CO_2 too.

Fig. 7 shows variations in macroporosity during gas sorption (uptake) experiments. The analysis of gas sorption on macropore porosity was performed considering the effects of only adsorption and, adsorption and absorption combined. We now observe the interplay of changes between a linear macropore volume expansion against the overburden stress and a nonlinear macropore decrease due to coal matrix swelling. In the case of N_2, at early stage when its concentration in coal is relatively low, the sorption related coal-swelling effect dominates the change in macroporosity and the macroporosity becomes smaller; at higher pressures, the macroporosity increases due to compression effects. This is not strictly the case, however, for CH_4 and, more importantly, for CO_2. The latter gas component has the potential to swell the solid material to an extent that macropore expansion due to gas uptake causes only leveling effect at large times. This is shown in Fig. 7 as a constant macroporosity value roughly equal to 1.5%.

Fig. 7 also illustrates the importance of absorption in microporous matrix during gas sorption in coal. Clearly, when absorption is included, the swelling of the coal matrix increases significantly. Especially, in the case of CO_2, as the adsorbed and dissolved gas amount in coal increases, porosity decreases even more. This can be a major concern during a CO_2-ECBM process.

3.3. Gas Transport in Bidisperse-Poroelastic Coal

The apparent diffusion coefficient values are calculated using Eq. (9a) and are shown in Fig. 8 during a CO_2 desorption exercise. For comparison with the poroelastic approach, the figure also shows gas transport in rigid coal bodies with a fixed macroporosity value, 2%. The diffusion coefficient shown in this graph is in dimensionless form, normalized using macropore diffusion coefficient, D_p. Hence, in the absence of gas transport in the microporous solid, i.e, the sorption processes and sorbed gas diffusion, its value is significantly larger and equal to 1.0, (unipore diffusion). The estimated values during gas release in bidisperse coals, on the other hand, point to a drastic deviation from this unity, values varying as low as 0.01 (Fig. 8). It drops significantly during an early transition period, when free gas in the macropores is rapidly released and depleted; and later, under the influence of microporous solid resistances (sorption and surface diffusion), it stabilizes to a constant low value prior to the complete gas recovery.

Fig. 8 shows that the stabilized value of the apparent diffusivity with respect to the macropore diffusivity is as low as 0.01. Yi et al. (2008) presented a comparative investigation of the overall transport using rigid bidisperse and unipore coal models. They showed that retardation due to sorption in microporous solid is mainly responsible for this significant drop in the stabilized effective diffusivity. Based on the parameters describing their gas–coal system, they also estimated an additional 20% drop in the stabilized effective diffusivity solely due to the presence of surface diffusion in the microporous solid.

Fig. 8 also shows the difference in gas transport in rigid and poroelastic coal bodies. It is clear that changing macropore and solid volumes cause an improvement on gas release, although the effect is almost negligible when compared with the diffusional and sorption resistances in microporous solids.

4. Conclusions

The theoretical framework considers macropores as the places where rapid mass transport takes place, whereas the microporous matrix as poroelastic solid coal bodies retaining majority of the gas in sorbed (physically adsorbed and dissolved) states. Behavior of the sorbed gas is then limited by the transport and equilibrium sorption in the solid. The approach introduces a bimodal pore structure to the framework in a simple mathematical form that defines gas mass accumulation and diffusive mass flux terms for each mode. This gives an ability and significant flexibility to investigate gas–solid interactions for a given initial- and boundary-value problem.

It is theoretically observed that gas sorption and transport processes and their influence on solid and macropore volumes are at a fundamental level closely related to the affinity of coal material to the natural gas component. Based on the conceptual model assumptions inherent to the numerical experiments performed, the following conclusions are made:

- Keeping the overburden stress constant, coal with a large sorption capacity shrinks during the gas release, consequently its macropore volume increases;
- Similarly, coal with a large sorption capacity swells during the gas uptake, yielding lower macroporosity values.
- As the sorption capacity decreases, or when the coal body consists of a spatially nonuniform material content with varying preferential affinity for the gas, it becomes a difficult task to determine the impact of gas release and uptake on the macroporosity at a given location in time.
- The importance of absorption in microporous matrix during the gas sorption in coal is illustrated explicitly. Clearly, when absorption is included, the swelling of the coal matrix increases. Especially, in the case of CO_2, macroporosity decreases even more as the adsorbed and dissolved gas amount in coal increases. This is proven to be a major concern during a CO_2-ECBM process in pilot field studies.
- The dynamic nature of poroelastic coal pore structure, however, is anticipated to a have a negligible influence on the overall gas mass transport during the gas production and sequestration operations. However, the impact of matrix-shrinkage/swelling on cleat porosity and, hence, fracture transport is well documented.

Nomenclature

a_i	quantities defined in Eq. (3)
c	nondimensional macropore concentration
c_μ	nondimensional micropore concentration
b	Langmuir isotherm constant (cm^3/mol)
C	macropore concentration (mol/cm^3)
C_o	initial macropore concentration (mol/cm^3)
$C_{\mu o}$	sorbed concentration in equilibrium with C_o (mol/cm^3)
C_μ	microporous solid-phase concentration (mol/cm^3)
$C_{\mu S}$	maximum sorbed-phase concentration in Langmuir isotherm (mol/cm^3)
D	apparent diffusion coefficient (cm^2/s)
De	Deborah Number
D_s	micropore (solid) diffusion coefficient (cm^2/s)
D_p	macropore diffusion coefficient (cm^2/s)
k'_d	Henry's constant
K	bulk modulus (Pa)
M	constrained axial modulus, (Pa)
n	shape factor
R	gas constant (J/K-mol)
T	temperature (K)
r	dimensionless radial coordinate
t	real time coordinate
x	dimensional radial coordinate

Greek symbols

α	macromolecular structural relaxation time
θ	characteristic diffusion time in micropores
τ	nondimensional time
γ	grain compressibility (1/Pa)
λ	dimensionless Langmuir isotherm nonlinearity parameters
ϕ	macroporosity

ε	ratio of sorbed phase to macropore flux
ε_l	dimensionless adjustment parameter
δ_1	nondimensional macropore capacity
δ_2	nondimensional microporous solid phase capacity

Acknowledgement

This research was partially funded by Natural Science Foundation of Chongqing, CNSFC, China, and by the Natural Science and Engineering Research Council of Canada, NSERC. Here, we gratefully acknowledge their financial contributions.

References

Chan, A.H., Koros, W.J., Paul, D.R., 1978. Analysis of hydrocarbon–gas sorption and transport in ethyl cellulose using dual sorption-partial immobilization models. Journal of Membrane Science 3, 117–130.

Clarkson, C.R., Bustin, R.M., 1999a. The effect of pore structure and gas pressure upon the transport properties of coal. 1 Isotherms and pore volume distributions. Fuel 78, 1333–1344.

Clarkson, C.R., Bustin, R.M., 1999b. The effect of pore structure and gas pressure upon the transport properties of coal. 2 Adsorption rate modeling. Fuel 78, 1345–1362.

Clarkson, C.R., Jordan, C.L., Gierhart, R.R., Seidle, J.P., 2008. Production data analysis of coalbed–methane wells. SPE Reservoir Evaluation Engineering 311–325.

Cohan, L.H., 1938. Sorption hysteresis and the vapor pressure of concave surfaces. Journal of American Chemical Society 60, 433–435.

Cui, X.J., Bustin, R.M., 2005. Volumetric strain associated with methane desorption and its impact on coalbed gas production from deep coal seams. American Association of Petroleum Geologists Bulletin 89, 1181–1202.

Cui, X.J., Bustin, R.M., Dipple, G., 2004. Selective transport of CO_2 and CH_4 in coals: insights from modeling of gas adsorption data. Fuel 83, 293–303.

Erb, A., Paul, D.R., 1981. Gas sorption and transport in polysulfone. Journal of Membrane Science 8, 11–22.

Gan, H., Walker, P.L., Nandi, S.P., 1972. Nature of porosity in American coals. Fuel 51, 272.

Gierhart, R.R., Clarkson, C.R., Siedle, J.P., 2007. Spatial variation of San Juan basin fruitland coalbed methane pressure dependent permeability: magnitude and functional form. Paper, IPTC 11333 presented at the International Petroleum Technology Conference, Dubai, U.A.E.

Green, T.K., Selby, T.D., 1994. Pyridine sorption isotherms of Argonne premium coals — dual-mode sorption and coal microporosity. Energy Fuels 8, 213–218.

Harpalani, S., Schraufnagel, R.A., 1990. Influence of matrix shrinkage and compressibility on gas production from coalbed methane reservoirs. Society of Petroleum Engineers paper, SPE 20729 presented at the SPE Annual Technical Conf. and Exhibition, New Orleans.

Higham, D.J., Higham, N.J., 2005. Matlab Guide. Society for Industrial and Applied Mathematics publication, Philadelphia.

Hui, C.-Y., Wu, K.-C., Lasky, R.C., Kramer, E.J., 1987. Case II diffusion in polymers. 2. Steady-state front motion. Journal of Applied Physics 61, 5137–5149.

Karacan, C.O., 2003. Heterogeneous sorption and swelling in a confined and stressed coal during CO_2 injection. Energy Fuels 17, 1595–1608.

Koros, W.J., Chan, A.H., Paul, D.R., 1977. Sorption and transport of various gases in polycarbonate. Journal of Membrane Science 2, 165–190.

Larsen, J.W., 2004. The effects of dissolved CO_2 on coal structure and properties. International Journal of Coal Geology 57, 63–70.

Mavor, M.J., Gunter, W.D., 2006. Secondary Porosity and Permeability of Coal vs. Gas Composition and Pressure. SPE Reservoir Evaluation Engineering 9, 114–125.

Mazumder, S., Bruining, J., 2007. Anomalous diffusion behavior of CO_2 in the macromolecular network structure of coal and its significance for CO_2 sequestration. Society of Petroleum Engineers paper SPE 109506 presented at the SPE Asia Pacific Oil & Gas Conference, Jakarta, Indonesia.

Medek, J., Weishauptova, Z., Kovar, L., 2006. Combined isotherm of adsorption and absorption on coal and differentiation of both processes. Microporous and Mesoporous Materials 89, 276–283.

Neogi, P., 1983. Anomalous diffusion of vapors through solid polymers. American Institute of Chemical Engineers Journal 29, 829–833.

Palmer, I., Mansoori, J., 1998. How permeability depends on stress and pore pressure in coalbeds: a new model. SPE Reservoir Evaluation Engineering 1, 539–544.

Paul, D.R., 1979. Gas sorption and transport in glassy-polymers. Physical Chemistry Chemical Physics 83, 294–302.

Rangarajan, R., Mazid, M.A., Matsuura, T., Sourirajan, S., 1984. Permeation of pure gases under pressure through asymmetric membranes — membrane characterization and prediction of performance. Industrial and Engineering Chemistry Process Design and Development 23, 79–87.

Ruckenstein, E., Vaidyanathan, A.S., Youngquist, G.R., 1971. Sorption by solids with bidisperse pore structures. Chemical Engineering Science 26, 1305–1318.

Romanov, V.N., Goodman, A.L., Larsen, J.W., 2006. Errors in CO_2 adsorption measurements caused by swelling. Energy Fuels 20, 415–416.

Seidle, J.P., Jeansonne, M.W., Erickson, D.J., 1992. Application of matchstick geometry to stress-dependent permeability in coals. Society of Petroleum Engineers paper SPE 24361 presented at the SPE Rocky Mountain Regional Meeting, Casper, Wyoming.

Shi, J.Q., Durucan, S., 2003. A bidisperse pore diffusion model for methane displacement and desorption in coal by CO_2 injection. Fuel 82, 1219.

Shi, J., Durucan, S., 2005. A model for changes in coalbed permeability during primary and enhanced methane recovery. SPE Reservoir Evaluation Engineering 8, 291–299.

Shimuzu, K., Takanohashi, T., Masahi, I., 1998. Sorption behaviours of various organic vapours to Argonne premium coal samples. Energy Fuels 12, 891–896.

Smith, D.M., Williams, F.L., 1984. Diffusion-models for gas-production from coal — determination of diffusion parameters. Fuel 63, 256–261.

Thimons, E.D., Kissel, F.N., 1973. Diffusion of methane through coal. Fuel 52, 274–280.

Thomas, N.L., Windle, A.H., 1982. A theory of Case II diffusion. Polymer 23, 529–542.

Unsworth, J.F., Fowler, C.S., Jones, L.F., 1989. Moisture in coal 2. Maceral effects on pore structure. Fuel 68, 18–26.

Vrentas, J.S., Duda, J.L., 1977. Diffusion in polyme-solvent systems. 3. Construction of Deborah number diagrams. Journal of Polymer Science. Part B, Polymer Physics 15, 441–453.

Vrentas, J.S., Jarzebski, C.M., Duda, J.L., 1975. Deborah number for diffusion in polyme-solvent systems. American Institute of Chemical Engineers Journal 21, 894–901.

Yi, J., Akkutlu, I.Y., Deutsch, C.V., 2008. Gas transport in bidisperse coal particles: investigation for an effective diffusion coefficient in coalbeds. Journal of Canadian Petroleum Technology 47 (10), 1–7.